

FABRICATION OF PHOSPHOR THIN FILM BY SURFACE MODIFICATION FOR PHOTONICS

D. S. Bae^{1*}, K. J. Jeong¹

¹Department of Convergence Materials Science & Engineering, Changwon National Univ., Gyeongnam, 641-773, South Korea
*dsbae7@changwon.ac.kr

Keywords: Phosphor, Thin Film, Core-Shell, Tb doped SiO₂

Abstract

Tb doped SiO₂ nanoparticles have been synthesized using a reverse micelle technique combined with metal alkoxide hydrolysis and condensation. The average size of synthesized Tb doped SiO₂ nanoparticles was about in the size range of 20-40 nm and core particles(Tb) 1-5 nm. Coating of Tb doped SiO₂ were prepared on glass substrate using TMOS, TEOS and MTES by sol-gel process. The resulted phosphors were characterized by UV-vis, FT-IR and TEM. The photoluminescence(PL) property of Tb doped SiO₂ phosphors was investigated. Upon excitation with ultraviolet(UV) irradiation, it is shown that there are emission peak at 480nm corresponding to the forced electric dipole ⁵D₃-⁷F₆ transition of Tb³⁺, respectively.

1 Introduction

During the past decades, doping has been extensively applied for the fabrication of hybrid materials with desirable properties and functions in modern materials science and engineering [1-10]. For rare earth based luminescent materials, doping is of fundamental importance in achieving and modifying the optical properties due to their abundant emission colors based on their unique 4f-4f or 4f-5d transitions [11-15]. The 4f emission spectra of rare earth ions are characterized by narrow lines with high color purity due to the shielding of 4f electrons by outer 5s and 5p electrons [11]. Furthermore, the host lattice has little influence on the positions of the 4f configuration energy levels, which are almost the same as the free ion levels. These special properties are widely employed to develop novel fluorescent materials with narrow emission lines, which exhibit potential applications in the fields of luminescent devices, optical transmission, biochemical probes, and medical diagnostics [16-20].

Inorganic phosphors have been widely investigated and used for many display and lighting devices such as cathode ray tubes (CRTs), plasma display panels (PDPs), field emission displays (FEDs), electroluminescence devices (ELDs), white light-emitting diodes (LEDs), and general fluorescence lamps [21,22]. Because the inorganic phosphors play an important role of emitting visible lights in each device, performances of the device are strongly depended on the luminescence properties of the phosphors used. The crystallite/particle size of the phosphor is one of the most important factors, which determine the luminescence properties, and many researchers have investigated the effects of the crystallite/particle size on the luminescence properties [23-27].

Compounds containing optically active lanthanide ions, e.g. Eu³⁺ and Tb³⁺, have long been used as phosphors and laser materials because of their sharp and intense emissions based on f-

f electronic transitions. Among such trivalent lanthanides, The Tb³⁺ ion has four narrow emission lines corresponding to ⁵D₄-⁷F_j transitions, where j = 2, 3, 4 and 5, and the strongest line for the transition ⁵D₄-⁷F₅ is observed at about 540nm as a green emission light with high purity [28].

For the core-shell structured particles, the structure, size and composition can be easily altered in a controllable way to tailor their functions [29]. Core-shell structured particles can preserve their unique magnetic, optical, and electronic properties when the surface of the nanoparticles is coated with silica [30,31]. By using silica spheres as a core and functional material particles (metal oxide, metal) as the shell, a broad range of hybrid materials with novel properties may result [32]. Spherical SiO₂ particles have been coated with rare-earth functional material layers, by a Pechini sol-gel process. The advantages of the core-shell structured phosphors prepared by this process include the easy availability of homogeneous spherical morphology in different size, decreased cost and its wide practicality for other phosphor materials [33]. Many routes have been explored to fabricate such core-shell particles, such as using co-precipitation [34], layer-by-layer self-assembly [35], surface reaction [36], sol-gel process [37] and MOCVD [38], etc.

In most cases, however, the degree of surface coverage is low and the coating is not uniform. The sol-gel process is an effective method for preparing such materials since the reactants can be homogeneously mixed at molecular level in solution. In most of the above cases, the sol-gel precursors used are metal alkoxides and/or organometallic compounds, which suffer from high cost, toxicity, and difficulty in controlling the experimental processes [39]. In general, annealing is required to improve the quality of the matrix containing the rare-earth oxide and to remove the -OH moieties, which are responsible for luminescence quenching. Hence, careful consideration of a suitable temperature is required in order to reach a good compromise between the reduction of quenching centers while maintaining accessible -OH groups on the silica surface, which can be functionalized.

In the research, the silica-based composite materials incorporating terbium nitrate complexes were prepared according to the reverse micelle and sol-gel method and their luminescence properties studied.

2 Materials and testing methods

2.1 Preparation of Tb doped SiO₂ solution

Microemulsions of total volume 20 ml consisting of 4 g of Igepal, 10 ml of cyclohexane, 0.65-1.30 ml of 0.02 M Tb(NO₃)₃·5H₂O solution. The average of the synthesized particles was controlled by varying the ratio R=[water]/[surfactant]. The microemulsion was mixed rapidly, and after 30 min of equilibration, one drop (~0.05 ml) of hydrazine hydrate (9 M N₂H₄·xH₂O, Aldrich Chemical Co.) was added as a reducing agent. After nanosize water droplets formed while stirring, TEOS was added into the stirred microemulsion. The amount of it was varied according to the different molar ratios of water to TEOS, H= [water]/[TEOS], which is the most important factor dictating the size of the nanoparticle. NH₄OH was injected into the microemulsion to accelerate the condensation reaction of metal alkoxide precursors. Reverse micelles were prepared from a nonionic surfactant, poly (oxyethylene) nonylphenyl ether (Igepal CO-520, Aldrich Chemical Co.), which was used without further purification. Other chemicals, such as tetraethoxysilane (TEOS, Aldrich Chemical Co.), cyclohexane, isoctane, and NH₄OH(28%) were used as received. The reacted products were aging for 12 hours and then washing was performed for a minimum of five times in ethanol. The structure, size and morphology of the resulting composite nanoparticles were examined by transmission electron microscope(TEM). For TEM studies, samples were prepared by adding drops of freshly prepared cluster solution on a carbon film supported on a Cu grid. The photoluminescence(PL) property of Tb/SiO₂ phosphors was investigated.

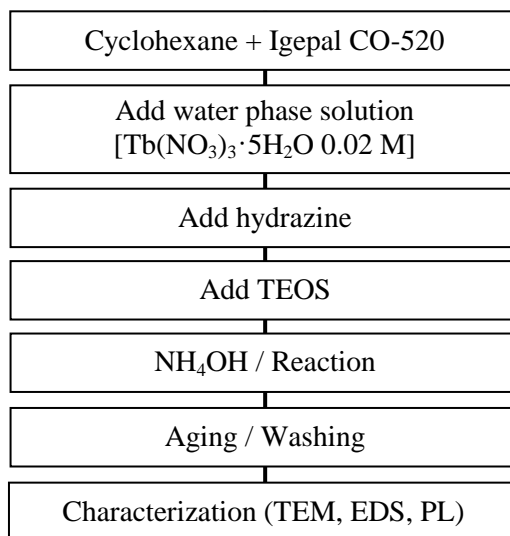


Figure 1. Flow chart for the synthesis of the Tb doped SiO₂ nanoparticles by a reverse micelle and sol-gel processing.

2.2 Preparation of coating solution

The coating solution were prepared using Tb/SiO₂ colloidal solution, deionized water and silane materials (TMOS, TEOS and MTES). The 10 ml of H₂O was added to 30 ml of Tb/SiO₂ colloidal solution (R=8, H=100, X=1). And then, silane materials (0.3 ml) was added at ambient temperature. The resultant solution was vigorously stirred at a rate of 200 rpm for 1 h.

2.3 Preparation of Thin films

The prepared coating sols were deposited on the surface of glass substrates using spin coating techniques. The spin coating was performed as follows. 1 drops of sol were placed on the surface substrates under rotaion 2000 rpm for 1 min. The coated substrates were dried at 80 °C in oven. Finally, the Tb/SiO₂ spin-coated samples after heat treatment at 200 °C for 2 h. All films appeared optically transparent.

2.4 Characterization of the thin films

FT-IR spectra of samples were obtained by a NICOLET 308 (Thermo Scientific) spectrometer by making their pills in KBr as a medium. The pressed disk containing 2 mg of the sample and 200 mg of fine grade Kbrwas scanned at wavenumber range of 400-4000 cm⁻¹. The thickness of the coating layers were evaluated with help of FE-SEM (MIRA II LMH). And also, The photoluminescence(PL) property of Tb/SiO₂ spin-coated phosphors was investigated.

3 Results

Ternary systems of Cyclohexane/Igepal CO-520/water offer certain advantages: they are spheroidal and monodisperse aggregates where water is readily solubilized in the polar core, forming a 'water pool' characterized by the ratio of water to surfactant concentration. Another important property of reverse micelles is their dynamics character; the water pools can exchange their contents by a collision process. The aggregation and self-assembly of the metal/surfactant/water species is complex, and very little is known about the cluster growth and final nano-structure as a function of synthesis conditions. The molar ratio of water to surfactant can determine the size of the micro-emulsion water core [40]. Therefore, the

diameter of the nanoparticles in the micro-emulsion can be controlled by the water/surfactants molar ratio(R) value.

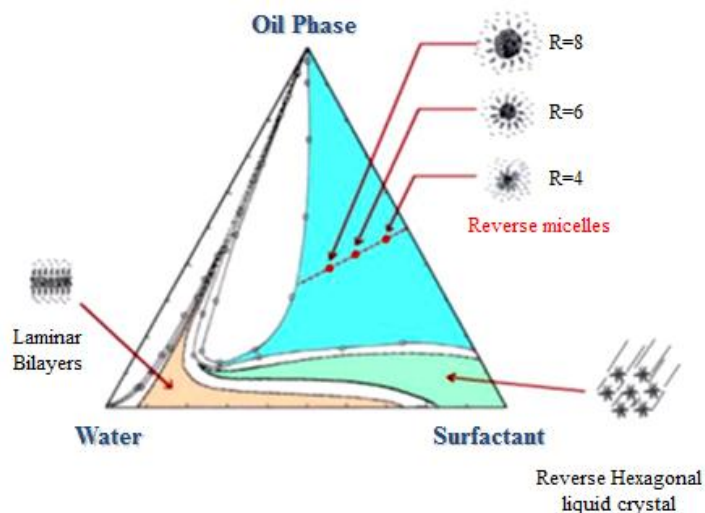


Figure 2. Phase diagram of surfactant-water-oil system [41].

Tb/SiO₂ composite nanoparticles were obtained in reverse micelles followed by in situ hydrolysis and condensation in the microemulsion. Fig. 3 shows spherical Tb/SiO₂ nanometer sized composite particles with a narrow size distribution were obtained in reverse micelles followed by in-situ hydrolysis and condensation in the micro-emulsion. The core particles are formed by a homogeneous nucleation and growth process, the shells are most likely formed through heterogeneous nucleation and growth. These two steps are different in mechanism, controlling the formation of the composite nanoparticles is very sensitive to modest processing changes. The first step is rapid, complete reduction of the metal to the zero valence state. The second step is growth via reagent exchanges between micelles [42].

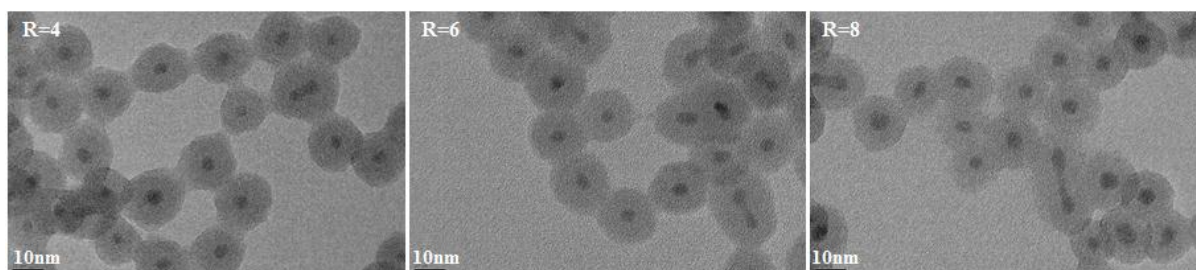


Figure 3. TEM micrographs of Tb/SiO₂ nanoparticles synthesized by a reverse micelle and sol-gel process as function of R values (C=0.02M, H=100, X=1).

Nucleation and growth of Tb particles is likely to be a diffusion-controlled process through interaction between micelles, but it may be influence by many other factors such as phase behavior and solubility, average occupancy of reacting species in the aqueous pool, and the dynamic behavior of the micro-emulsion [42].

As a first approximation, it may be assumed that the reverse micelle aggregates present in the solution are not affected by the addition of TEOS molecules or by subsequent reactions, and in particular that the aggregation numbers of the micelles remain unchanged. The TEOS alkoxide molecules would then interact rapidly with the water molecules inside the reverse micelles, forming partially hydrolyzed species. These hydrolyzed species remain bound to the

micelles due to their enhanced amphiphilic character brought about by the formation of silanol groups. It is likely that hydrolysis occurs within each reverse micelle, whereas condensation (particle growth) may occur also by intermicellar contracts. Therefore, the size of the composite particles depends on the relative rates of the hydrolysis and condensation reactions. Fig. 4 shows the spectrum of Tb/SiO₂ composite nanoparticles by TEM-EDS analysis. The core particles appear Tb pattern peaks and the shells appear SiO₂ pattern peaks.

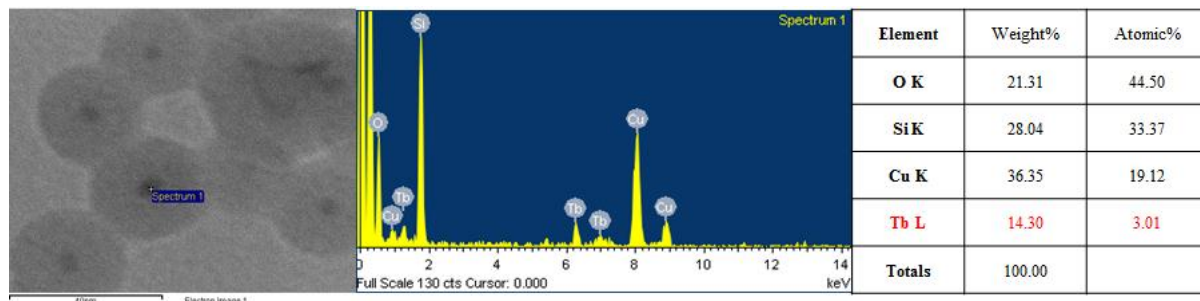


Figure 4. TEM-EDS analysis of Tb/SiO₂ nanoparticles synthesized by a reverse micelle and sol-gel process as function of R values (C=0.02M, H=100, X=1).

The coating of self-assembled particles can be tailorable by alternating the mole ratio of water to silane. This design is an alterable method to prepare the nano-structured coating. In our experiment, the alteration of coating of self-assembled nanoparticles in stepwise-diluted sol solutions with varied types of silane was investigated. The self-assembled coating is obtained by crosslinking the molecules formed by TMOS, TEOS and MTES.

Spin-coating method is a simple and cheap oxide thin-film deposition technique, but it requires soluble reagents. It is possible to control the film thickness by merely adjusting the solution viscosity or coating times. Cross-sectional SEM micrographs of the Tb doped SiO₂ thin films are shown in Fig. 5(a), (b) and (c), respectively.

The FE-SEM micrographs of Silane doped Tb/SiO₂ thin film that show its average thickness to be about 30 nm and obviously improves the surface flatness and enhances uniformity of film thickness. It also has a transparent thin film layer. But, the surface Fig. 5(a) and (c) than (b) is slightly irregular.

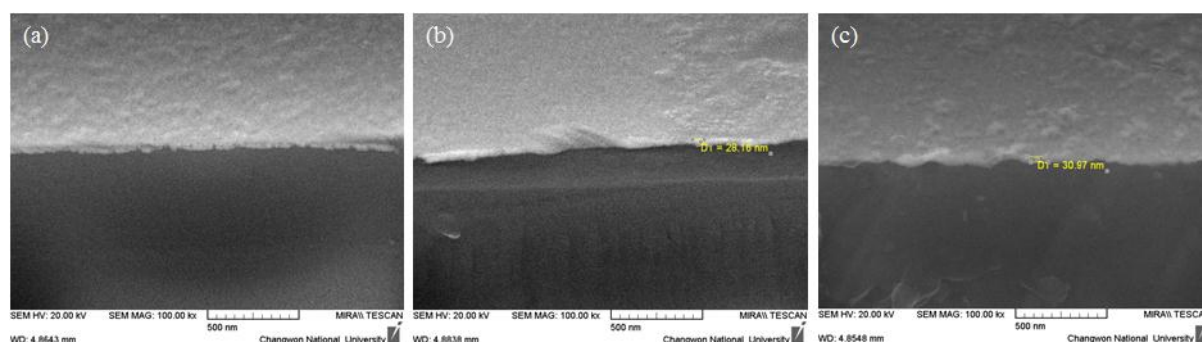


Figure 5. FE-SEM images of thickness of coating layer by spin-coating method (a=TMOS, b=TEOS and c=MTES).

Fig. 6 shows the FT-IR spectra of the standard sol solution and the spin-coated thin films. As shown in Fig. 6, there was a peak at 3406 cm⁻¹ related to hydroxyl group. The band near 2923 cm⁻¹ was related to the epoxide groups and was due to the stretching CH₂. The distinct band at 1096 cm⁻¹ was the characteristic of stretching of Si-O-Si. The band at 908 cm⁻¹ was due to the stretching of Si-OH. After coated, the peaks at 1730, 1633 and 2133 cm⁻¹ were appeared that

associated with the C=O, C≡N. From among these, FT-IR spectra appeared most strongly when TEOS was added.

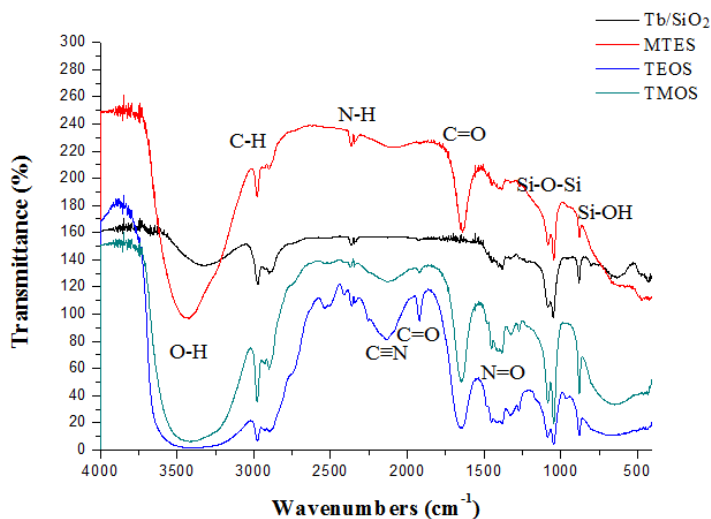


Figure 6. FT-IR transmittance spectra of Tb/SiO₂ thin films after heat treatment at 200 °C for 2 h.

The luminescent spectra of trivalent lanthanide ions in phosphors are mainly from two types of electronic transitions: 4f-4f transition and 5d-4f transition. The former generally shows sharp emission line, while the latter have a broad band character. The PL properties of Tb/SiO₂ thin film phosphors were characterized by emission spectra, as shown in Fig. 7.

The emission spectra of the obtained sample which were measured under 238 nm excitation at the room temperature. The sharp emission peaks originates from the 4f-4f transition of Tb³⁺ ions : ⁵D₃-⁷F₆ (480 nm, blue) in all samples. One of the main emission peaks in Tb³⁺ ions : ⁵D₄-⁷F₅ (543 nm, green) was not observed. And the addition of TEOS thin film samples was found to be the highest emission intensity.

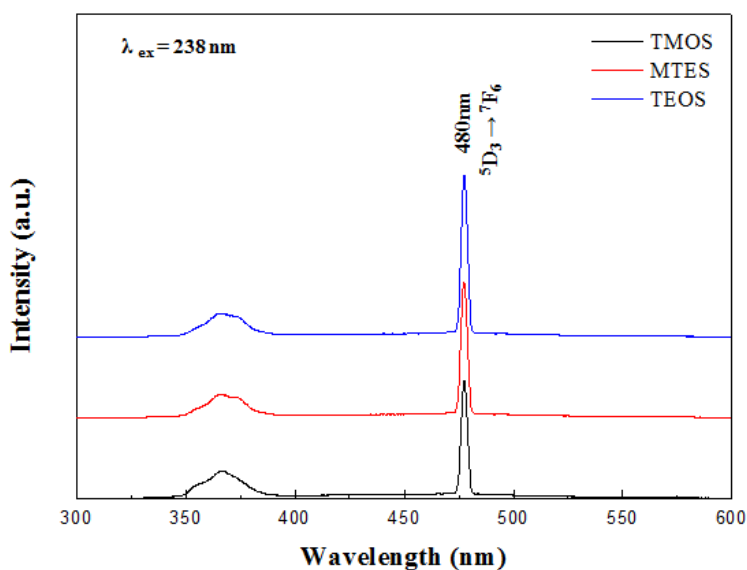


Figure 7. PL emission spectra of Tb/SiO₂ thin films after heat treatment at 200 °C for 2 h.

4 Conclusion

The Tb/SiO₂ thin films were deposited on glass substrates at low temperatures using a simple sol-gel spin-coating method. The synthesized Tb doped SiO₂ solution by a reverse micelle and sol-gel processing, with a uniform size distribution have been prepared using self-assembly molecules, in conjunction with the hydrolysis and condensation of organometallic precursors. The average size and size distribution of the synthesized Tb doped SiO₂ particles were about 2 nm(core), 25 nm(shell) and broad, respectively. The shape of the synthesized particles was spherical.

Coating solution was prepared by adding the silane (TMOS, TEOS and MTES). The result of coating on the glass substrates by using the silane and coating layer were well uniformly made. The thickness of the thin film layer was nearly similar. FT-IR results proved the changes of chemical groups by silane structure in thin film samples. Upon excitation with ultraviolet(UV) irradiation, it is shown that there are emission peak at 480nm corresponding to the forced electric dipole ⁵D₃-⁷F₆ transition of Tb³⁺, respectively

Acknowledgment

This work was supported by the National Research Foundation of Korea(NRF) grant funded by the Korea government (MEST) (No. 2011-0004448).

References

- [1] Y.F. Zhu, H.G. Pan, M.X. Gao, J.X. Ma, Y.Q. Lei, Q.D. Wang. *Int. J. Hydrogen Energy*, **28**, pp. 311, (2003).
- [2] H.G. Pan, R. Li, Y.F. Liu, M.X. Gao, H. Miao, Y.Q. Lei, Q.D. Wang. *J. Alloys Compd*, **463**, pp. 189, (2008).
- [3] Y.F. Liu, K. Luo, Y.F. Zhou, M.X. Gao, H.G. Pan. *J. Alloys Compd*, **481**, pp. 473, (2009).
- [4] M. Gao, H. Miao, Y. Zhao, Y.F. Liu, H.G. Pan. *J. Alloys Compd*, **484**, pp. 249, (2009).
- [5] J.H. Wang, J.J. Hu, Y.F. Liu, Z.T. Xiong, G.T. Wu, H.G. Pan, P. Chen. *J. Mater. Chem*, **19**, pp. 2141, (2009).
- [6] H.G. Pan, F.M. Yang, C.P. Chen, N. Tang, X.F. Han, Q.D. Wang. *J. Magn. Magn. Mater*, **163**, pp. 221, (1996).
- [7] L.X. Chen, Y.Q. Lei, G.M. Zhu, H.G. Pan, K. Ren, Z.Z. Li, X.G. Yang, Q.D. Wang. *J. Alloys Compd*, **684**, pp. 293–295, (1999).
- [8] B. Kotur, O. Myakush, H. Michor, E. Bauer. *J. Alloys Compd*, **299**, pp. 135 (2010).
- [9] X.D. Feng, D.C. Sayle, Z.L. Wang, M.S. Paras, B. Santora, A.C. Sutorik, T.X.T. Sayle, Y. Yang, Y. Ding, X.D. Wang, Y.S. Her. *Science* **312**, pp. 1504, (2006).
- [10] Y.A. Yang, O. Chen, A. Angerhofer, Y.C. Cao. *J. Am. Chem. Soc.* **128**, pp. 12428, (2006).
- [11] G. Blasse, B.C. Grabmaier. *Springer-Verlag*, Berlin, Heidelberg, (1994).
- [12] F. Wang, Y. Han, C.S. Lim, Y.H. Lu, J. Wang, J. Xu, H.Y. Chen, C. Zhang, M.H. Hong, X.G. Liu. *Nature*, **463**, pp. 1061, (2010).
- [13] T. Justel, H. Nikol, C. Ronda. *Angew. Chem. Int. Ed*, **37**, pp. 3085, (1998).
- [14] F. Auzel. *Chem. Rev*, **104**, pp. 139, (2004).
- [15] E. Downing, L. Hesselink, J. Ralston, R. Macfarlane. *Science* **273**, pp. 1185, (1996).
- [16] X. Wang, J. Zhuang, Q. Peng, Y.D. Li. *Nature*, **437**, pp. 121, (2005).
- [17] R. Si, Y.W. Zhang, L.P. You, C.H. Yan. *Angew. Chem. Int. Ed*, **44**, pp. 3256, (2005).
- [18] K. Kompe, H. Borchert, J. Storz, A. Lobo, S. Adam, T. Moller, M. Haase. *Angew. Chem. Int. Ed*, **42**, pp. 5513, (2003).
- [19] T. Yu, J. Joo, Y.I. Park, T. Hyeon. *J. Am. Chem. Soc.* **128**, pp. 1786, (2006).
- [20] J.W. Stouwdam, F. van Veggel. *Nano Lett*, **2**, pp. 733, (2002).

- [21] G. Blasse, B.C. Grabmaier. *Luminescence Materials*, Springer, Berlin, (1994).
- [22] S. Shionoya, W.M. Yen. *Phosphor Handbook*, CRC press, New York, (1997).
- [23] G. Wakefield, E. Holland, P.J. Dobson, J.L. Hutchison. *Adv. Mater*, **13**, pp. 1557, (2001).
- [24] W. Wang, W. Widiyastuti, T. Ogi, I.W. Lenggoro, K. Okuyama. *Chem. Mater*, **19**, pp. 1723, (2007).
- [25] H.S. Yoo, H.S. Jang, W.B. Im, J.H. Kang, D.Y. Jeon. *J. Mater. Res*, **22**, pp. 2017, (2007).
- [26] A. Vecht, C. Gibbons, D. Davies, X. Jing, P. Marsh, T. Ireland, J. Silver, A. Newport. *J. Vac. Sci. Technol. B*, **17**, pp. 750, (1999).
- [27] X. Jing, T. Ireland, C. Gibbons, D.J. Barber, J. Silver, A. Vecht, G. Fern. *J. Electrochem. Soc*, **146**, pp. 4654, (1999).
- [28] S. Hüfner. *Optical Spectra of Transparent Rare Earth Compounds*, Academic Press, New York, (1978).
- [29] A.E. Neeves, M.H. Birnboim. *J. Opt. Soc. Am. B*, **6**, pp. 787, (1989).
- [30] Y.H. Deng, D.W. Qi, C.H. Deng, X.M. Zhang, D.Y. Zhao. *J. Am. Chem. Soc*, **130**, pp. 28, (2008).
- [31] T. Zhai, Z. Gu, Y. Dong, H. Zhong, Y. Ma, H. Fu, Y. Li, J. Yao. *J. Phys. Chem. C*, **111**, pp. 11604, (2007).
- [32] Y. Kobayashi, M.A. Correa-Duarte, L.M. Liz-Marzán. *Langmuir*, **17**, pp. 6375, (2001).
- [33] M. Yu, H. Wang, C.K. Lin, G.Z. Li, J. Lin. *Nanotechnology*, **17**, pp. 3245, (2006).
- [34] H. Giesche, E. Matijević. *J. Mater. Res*, **9**, pp. 436, (1994).
- [35] V. Salgueirino-Maceira, M. Spasova, M. Farle. *Adv. Funct. Mater*, **15**, pp. 1036, (2005).
- [36] A. Dokoutchaev, J.T. James, S. C. Koene, S. Pathak, G.K.S. Prakash, M.E. Thompson. *Chem. Mater*, **11**, pp. 2389, (1999).
- [37] R.A. Caruso, M. Antonietti. *Chem. Mater*, **13**, pp. 3272, (2001).
- [38] K.W. Chang, J.J. Wu. *Adv. Mater*, **17**, pp. 241, (2005).
- [39] M. Yu, J. Lin, Z. Wang, J. Fu, S. Wang, H.J. Zhang, Y.C. Han. *Chem. Mater*, **14**, pp. 2224, (2002).
- [40] Ph. Monnoyer, A. Fonseca, J. B. Nagy. *Colloid Surf. A: Physicochemical Eng. Aspects*, **100**, pp. 233, (1995).
- [41] Kunieda et al, *J. Col. and Inter. Sci*, **70**, pp. 581, (1979).
- [42] LI. T, MOON. J, MORRONE. A.A, MECHOLSKY. J.J, TALHAM. D.R, ADAIR. J.H. "Preparation of Ag/SiO₂ nanosize composites by a reverse micelle and sol-gel technique", *J. Langmuir*, **15**, pp. 4328-4334, (1999).